The role of telomere shortening in carcinogenesis: A hybrid stochastic-deterministic approach

Ignacio A. Rodriguez-Brenes [1,2,*], Natalia L. Komarova [1,2], and Dominik Wodarz [2,1]

[1]Department of Mathematics, University of California, Irvine, California, United States of America.

[2]Department of Ecology and Evolutionary Biology, University of California, Irvine, California, United States of America.

*Corresponding author.

Email: iarodrig@uci.edu (IR)

Abstract

Genome instability is a characteristic of most cancers, contributing to the acquisition of genetic alterations that drive tumor progression. One important source of genome instability is linked to telomere dysfunction in cells with critically short telomeres that lack p53-mediated surveillance of genomic integrity. Here we research the probability that cancer emerges through an evolutionary pathway that includes a telomere-induced phase of genome instability. To implement our models we use a hybrid stochastic-deterministic approach, which allows us to perform large numbers of simulations using biologically realistic population sizes and mutation rates, circumventing the traditional limitations of fully stochastic algorithms. The hybrid methodology should be easily adaptable to a wide range of evolutionary problems. In particular, we model telomere shortening and the acquisition of two mutations: Telomerase activation and p53 inactivation. We find that the death rate of unstable cells, and the number of cell divisions that p53 mutants can sustain beyond the normal senescence setpoint determine the likelihood that the first double mutant originates in a cell with telomere-induced instability. The model has applications to an influential telomerase-null mouse model and p16 silenced human cells. We end by discussing algorithmic performance and a measure for the accuracy of the hybrid approximation.

Introduction

Cancer is driven by a process of clonal evolution, which involves the sequential accumulation of mutations that ultimately allow for uncontrolled cell proliferation [1, 2]. Often, tumors develop different types of genome instability, which impact the tumor's ability to evolve and progress. One important source of genome instability is telomere dysfunction [3]. While mathematical modeling has significantly advanced our understanding of tumor evolution [4], the role of telomere shortening in connection to genome instability and carcinogenesis remains poorly understood from a quantitative perspective.

A serious obstacle in modeling tumor evolution in general, is that traditional fully stochastic algorithms, such as Gillespie's method [5], are ill-equipped to deal with population sizes that are biologically relevant to the study of tumorigenesis at the scale of cell populations. Moreover, the low mutation rates of mammalian cells require a very large number of simulations to obtain statistically meaningful results on mutant dynamics. As a consequence, too often models are constructed and analyzed with population sizes that are unrealistically small and mutation rates that are unrealistically large. This is especially problematic when trying to compare model results to emerging clinical data. Here we draw on ideas related to the development of hybrid stochastic-deterministic methods to circumvent the aforementioned limitations of fully stochastic approaches. In particular, we outline an efficient hybrid stochastic-deterministic algorithm that allows for the use of realistic population sizes and mutation rates. This algorithm should be easily adaptable to a wide range of applications in the field of evolution.

In this article, we develop a mathematical model that takes into account the effects of telomere shortening in a clonal cell population. It examines the relative likelihood and frequency of the order of acquisition of the two crucial mutations in carcinogenesis, telomerase activation and p53 inactivation, as a function of key biological parameters. We also present results on the probability that the first double mutant originates in a cell with genome instability caused by telomere dysfunction. This probability is particularly important because cells that undergo telomere-induced genome instability typically acquire a large number of genome abnormalities associated with cancer [6], which suggests that an evolutionary pathway that includes transient telomere deficiency can facilitate malignant progression [3]. To implement the model we used the hybrid stochastic-deterministic algorithm. We also discuss a measure for the accuracy of the hybrid approximation, and compare algorithmic performance to a fully stochastic implementation of the model.

Telomeres and telomere crisis

Telomeres are repetitive sequences of DNA found at the ends of linear chromosomes. They play a protective role by hiding the chromosome ends from the DNA damage response machinery. In cells that lack telomere maintenance pathways telomere length shortens with each cell division. If cell cycle checkpoints are intact, critically short telomeres halt cell proliferation, inducing either a terminal state of arrest called cellular senescence, or apoptosis [6]. Thus, normal cells that lack telomere maintenance pathways are only capable of a limited number of divisions, a phenomenon known as Hayflick's limit [7]. Telomerase is a ribonucleoprotein enzyme that extends telomere length. It is composed of a catalytic component that includes the protein TERT, and the RNA component TERC. Cells that express telomerase at sufficient levels offset the telomere shortening that occurs during cell division, which allows them to bypass replicative limits and divide indefinitely [3]. Since most mutations occur during cell division, replicative limits protect against cancer, by limiting the sequential accumulation of mutations and the clonal expansion of cells.

Failure of cells with critically short telomeres to undergo senescence can result in telomere crisis. During crisis continued telomere shortening leads to telomere dysfunction increasing the chance of non-homologous end joining (NHEJ) and the fusion of one dysfunctional telomere to another. Cells with fused telomeres become dicentric, which leads to breakage–fusion–bridge cycles, and high levels of genome instability and cell death [3]. Genome instability in cells undergoing crisis can give rise to chromosome gains and losses, gene amplifications and deletions, and non-reciprocal translocations amongst other types of genomic alterations. The rare cells that escapes crisis, usually through telomerase activation, typically harbor a large number of genomic abnormalities associated with cancer [6]. It has thus been suggested that the passage and emergence from crisis can be an important contributor to tumor development in some cancers [8].

In this article we use mathematical models to study the emergence and population dynamics of cells with two types of mutations: loss of p53 function and telomerase activation.

Inactivation of p53 is a frequent event in tumorigenesis [9]. And in particular, inactivation of the p53 pathway is necessary to bypass telomere-induced senescence [10]. In the paper we focus on the first emergence of a double mutant and in the order of acquisition of the two mutations. We model the effects of telomere crisis by assuming an elevated death rate for unstable (in crisis) cells. The order of mutations is important, because cells that undergo crisis can acquire a number of important genomic changes, which occur during the period of genome instability caused by telomere dysfunction.

Our model has a direct application to the important $\mathrm{TERC}^{-/-}$ mouse model. Mouse cells have very long telomeres and express telomerase promiscuously; as a consequence telomere shortening is not a barrier to tumor progression in mice [11]. To test the function of telomerase in tissue biology a telomerase-knockout mouse model was developed, by breeding mice that do not express TERC (the RNA component of telomerase). Continuous breeding of $\mathrm{TERC}^{-/-}$ mice over successive generations led to the progressive shortening of telomeres [12]. A series of studies were then conducted in late generation $\mathrm{TERC}^{-/-}$ mice, in which a gene (Ink4a/Arf) encoding for two distinct tumor suppressor proteins was deleted. Mice null for this gene develop sarcomas and lymphomas with short latency; $\mathrm{TERC}^{-/-}$ mice however, had reduced tumor incidence and increased latency, demonstrating that telomere shortening and lack of telomerase expression inhibits tumorigenesis in late generation $\mathrm{TERC}^{-/-}$ mice [13, 14].

Critically short mouse telomeres induce senescence by activating p53; and the loss of p53 function in mice is sufficient to bypass senescence [15]. Studies of $\mathrm{TERC}^{-/-}\,\mathrm{p53}^{+/-}$ mutant mice also revealed that the $\mathrm{p53}^{+/-}$ phenotype is sufficient to abrogate the normal growth arrest that occurs in response to short telomeres [16]. Neoplastic lesions in these mice had a large number of genomic aberrations consistent with telomere dysfunction and the breakage–fusion–bridge cycles that occur during crisis.

Our model also has applications to human cells that lack p16 function. In humans, stem cells, germ cells, and the vast majority of cancer cells ($\sim$ 90%) express telomerase,

whereas other cell types do not [17]. The critical component of telomerase that is missing in most human cells is the catalytic subunit TERT. Unlike murine cells, human cells can trigger senescence by activating the p53 or the p16/RB pathways [10]. Although there is also evidence that suggests that p16-induced senescence is not the direct consequence of telomere shortening [18]. Regardless, cells lacking p16 function may not be uncommon *in vivo* in humans, since epigenetic silencing of the p16 gene is commonly found in histologically normal human mammary epithelial cells (HMECs) [19]. Moreover, cell culture studies of HMECs repeatedly show that following the spontaneous silencing of p16, the rare cells that are able to bypass the p53 checkpoint undergo extended proliferation and eventually enter crisis [20, 21].

Model description

We consider four types of cells, which for notation purposes we call X, Y, Z, and W, see Figure 1A. At the base of the model we have X cells, which are telomerase negative (here noted as tmase–). Telomerase null cells correspond to TERC$^{-/-}$ cells in the context of the mouse model previously described, or TERT negative cells in the context of human somatic cells. X cells have two functioning p53 alleles (p53$^{+/+}$). These are proliferating cells at early possibly pre-neoplastic stages of tumor development. This characterization is consistent with the understanding that in certain tumors telomere crisis is a very early event. In breast cancer for example, telomere crisis is believed to occur during progression from usual ductal hyperplasia (UDH) to ductal carcinoma in situ (DCIS) [8]. Being telomerase negative, X cells can divide only a limited number of times. To model replicative limits we assume that each cell has a replication capacity $\rho \geq 0$. When a cell with replication capacity $\rho > 0$ divides, it produces two daughter cells with replication capacities $\rho - 1$. Cells with replication capacity $\rho = 0$ become senescent and stop dividing (Figure 1B). The maximum replication capacity in the model is denoted by ρ_{m}.

Y cells are telomerase positive (tmase+) and p53$^{+/+}$. Telomerase expression allows them

to escape replicative limits, making them capable of dividing an unlimited number of times. In the model, a Y cell arises from a point mutation in an X cell. Recently, activating point mutations in the tmase promoter have been identified in multiple cancer types [22, 23, 24, 25]. We consider mutations that occur during cell division and use the approximate point mutation rate in cancer $\mu_2 = 10^{-9}$ [26].

Z cells are p53$^{+/-}$ and telomerase negative. In mice, single-copy loss of p53 is sufficient to affect the cell's ability to undergo senescence in response to critically short telomeres [16]. Direct confirmation that these same dynamics occur in humans is currently missing. However, there is strong evidence that the human p53 gene is haplo-insufficient in a wide variety of contexts [27]. Furthermore, 80% of the most common p53 mutants have been found to have the capacity to exert a dominant-negative effect over wild-type p53 [9]. Hence, in the model we assume that the p53$^{+/-}$ phenotype allows cells to extend their replication capacity by ρ_e cell divisions beyond the point at which senescence occurs in normal cells. We call the parameter ρ_e the replication capacity extension. Early experiments, based on SV40-induced disruption of p53, suggest that the replication capacity extension is in the order of 20 PD [28], with a range of 20 to 30 PD being suggested [29]. The precise value of ρ_e however, is likely to vary *in vivo*; we thus treat it as a variable, and explore the effects of varying ρ_e on the system. In the model, Z cells arise from X cells with a rate per cell generation $\mu_1 = 10^{-7}$ (a common estimate for the rate per cell division of inactivating one copy of a tumor suppressor gene [30]).

W cells arise from Z cells that keep dividing past their extended replication capacity. As a consequence their telomeres continue to shorten, up to the point where they become dysfunctional, resulting in genome instability. Cells at this stage enter crisis, a phase characterized by non-homologous end joining, breakage–fusion–bridge cycles, and widespread cell death [3]. These dynamics are considered in the model by including a separate death rate, D, for W cells.

Breast and colorectal cancer studies suggest that telomere crisis is an early event [8, 31].

In colorectal cancer, there is evidence of telomere dysfunction during the adenoma–early carcinoma transition [31]. Moreover, in a study of colorectal adenomas with average size 2 mm (range 1–3 mm) 55% of adenomas showed evidence of chromosomal instability consistent with telomere dysfunction [32]. In breast cancer, crisis is believed to occur during the UDH to DCIS transition [8], and according to a standard diagnostic criterium, ductal hyperplasias should be less than 2 mm in diameter [33]. Avascular tumors can grow up to 2–3 mm in diameter [34]. Hence, these data suggest that telomere crisis might occur during the avascular phase of tumor development. Based on these observations we limit our study to events occurring during avascular growth.

If we use a 2–3 mm diameter for avascular tumors and the volume measurements for tumor cells reported in [35], we find that the maximum cell population of an avascular tumor ranges from 3.6×10^6 – 5.3×10^7 cells. In the article we choose the intermediate value, $N = 10^7$, for the maximum cell population size. To incorporate this limit in population size, we make the cell division rate dependent on cell density, controlled by the variable f in equation [1]. In equations [1–5], we define $K = 10^7/(1-d/r)$, where r and d are respectively the cell division and cell death rate parameters. This definition of K ensures that the maximum population size is equal to 10^7, irrespective of the magnitudes of r and d; it is thus consistent with our understanding that maximum population size in avascular tumors is limited by factors such as nutrient accessibility, and not by the relative magnitudes of the cell division and cell death rates. Finally, we note that r and the cell death parameters, d and D, have arbitrary units of 1/time. We can then express the model in dimensionless units of time by setting $r = 1$ in the simulations and expressing the values of d and D in relation to this value of r.

Double mutants can be generated through a $p53^{+/-}$ mutation in a Y cell (with rate μ_1) or through a tmase+ mutation in a Z or W cell (with rate μ_2). In the this article we are interested in the first emergence of a double mutant, for this reason when the first double mutation occurs the simulations stop. The ordinary differential equation representation of the model, including *only single* mutations (either tmase+ or $p53^{+/-}$) is given by equations

195 [1–5]:

$$f = (1 - tot/K) \quad , \quad tot = Y + W + \sum_{j=0}^{\rho_{\mathrm{m}}} X_j + \sum_{j=0}^{\rho_{\mathrm{m}}+\rho_{\mathrm{e}}} Z_j \tag{1}$$

$$\begin{cases} \dot{X}_{\rho_{\mathrm{m}}} &= -rX_{\rho_{\mathrm{m}}}f - dX_{\rho_{\mathrm{m}}} \\ \dot{X}_{\rho_{\mathrm{m}}-1} &= 2rX_{\rho_{\mathrm{m}}}f - rX_{\rho_{\mathrm{m}}-1}f - dX_{\rho_{\mathrm{m}}-1} - r(\mu_1+\mu_2)X_{\rho_{\mathrm{m}}}f \\ \dot{X}_{\rho_{\mathrm{m}}-2} &= 2rX_{\rho_{\mathrm{m}}-1}f - rX_{\rho_{\mathrm{m}}-2}f - dX_{\rho_{\mathrm{m}}-2} - r(\mu_1+\mu_2)X_{\rho_{\mathrm{m}}-1}f \\ &\vdots \\ \dot{X}_0 &= 2rX_1f - dX_0 - r(\mu_1+\mu_2)X_1f \end{cases} \tag{2}$$

$$\dot{Y} = rYf - dY + \mu_2 \sum_{j=1}^{\rho_{\mathrm{m}}} rX_j f \tag{3}$$

$$\begin{cases} \dot{Z}_{\rho_{\mathrm{m}}+\rho_{\mathrm{e}}} &= -rZ_{\rho_{\mathrm{m}}+\rho_{\mathrm{e}}}f - dZ_{\rho_{\mathrm{m}}+\rho_{\mathrm{e}}} \\ \dot{Z}_{\rho_{\mathrm{m}}+\rho_{\mathrm{e}}-1} &= 2rZ_{\rho_{\mathrm{m}}+\rho_{\mathrm{e}}}f - rZ_{\rho_{\mathrm{m}}+\rho_{\mathrm{e}}-1}f - dZ_{\rho_{\mathrm{m}}+\rho_{\mathrm{e}}-1} + \mu_1 rX_{\rho_{\mathrm{m}}}f \\ &\vdots \\ \dot{Z}_{\rho_{\mathrm{e}}} &= 2rZ_{\rho_{\mathrm{e}}+1}f - rZ_{\rho_{\mathrm{e}}}f - dZ_{\rho_{\mathrm{e}}} + \mu_1 rX_1 f \\ \dot{Z}_{\rho_{\mathrm{e}}-1} &= 2rZ_{\rho_{\mathrm{e}}}f - rZ_{\rho_{\mathrm{e}}-1}f - dZ_{\rho_{\mathrm{e}}-1} \\ &\vdots \\ \dot{Z}_0 &= 2rZ_1f - rZ_0f - dZ_0 \end{cases} \tag{4}$$

$$\dot{W} = rWf - DW + 2rZ_0f \tag{5}$$

In Eqs. [1–5] we assume that both offspring of a dividing cell cannot mutate simultaneously, since the probability of such an event occurring is negligible [30].

Hybrid method

Studying evolutionary processes computationally requires the ability to simulate the dynamics of large and small populations simultaneously. Mutations are stochastic and rare, and at least transiently, very small mutant populations can coexist with a large number of wild type individuals. In such settings, tracking the stochastic fluctuations of the small mutant populations can be essential to determine the final outcomes of the system. A problem then arises trying to simulate a multi-scale system stochastically, given that in classical fully stochastic algorithms, such as Gillespie's method, as the population size increases the average time step decreases [5]. Recently, and especially in the field of Physical Chemistry, novel computational approaches have been developed (e.g. the Next Reaction Method and Tau-Leaping methods [36, 37]), which try to address these difficulties. There is also an important push in the development of hybrid stochastic-deterministic approaches [38, 39]. These ideas however, have not significantly penetrated the studies of population dynamics and evolution, presumably because they can rely on theoretical concepts (e.g. Langevin's equation), which are not very common in these fields. Here, we present an application of these ideas to the field of evolution, by outlining a hybrid stochastic-deterministic algorithm for our model.

Intuitively, the implementation of the algorithm relies on two simple ideas: (i) mutations should be modeled stochastically; and (ii) if, a cell population is sufficiently large, an ODE representation can provide a good approximation of most stochastic trajectories of the population. With this idea in mind we begin with the system described in equations [1–5], which from now on we call the full system. We can write this system as a single vector equation $d\mathbf{V}/dt = \mathbf{F}(\mathbf{V})$, where $\mathbf{V}$ is a vector that contains all the different cell types. Let $M > 0$ be a given threshold. We can classify the X population as small if $\sum X_i < M$, or as large otherwise, and use the same criteria to classify the other cell types (W, Y and Z). At any given

time, let $\mathbf{V}_l$ and $\mathbf{V}_s$ be vectors containing the large and small cell populations. We can then define the reduced system $d\mathbf{V}_l/dt = \mathbf{F}_l(\mathbf{V}_l)$ derived from the full system by: (1) Retaining only the equations for the large cell populations $\mathbf{V}_l$; (2) keeping constant the contributions of the small populations $\mathbf{V}_s$; and (3) eliminating the mutation terms from the equations. If the $\mathbf{V}_l$ are sufficiently large, there will be a time interval $(t, t+\tau)$, where the deterministic solution of the reduced ODE will approximate the trajectories of the large populations in a stochastic implementation of the full system.

The events in the model are cell division, mutation, and death. In Gillespie's method, every event ν has a given propensity $a_\nu(\mathbf{V})$. The time at which the next event ν will occur is exponentially distributed with intensity $a_\nu(\mathbf{V})$. In the hybrid approach, cell division and death of large populations are modeled deterministically (using the reduced system), while cell division and death of small populations and all mutations are modeled stochastically, with propensities $a_\nu(\mathbf{V}_s, \mathbf{V}_l(t))$ that now vary continuously with time. Hence, the next occurrence of a stochastic event ν is a non-homogeneous Poisson process, with a time varying intensity $a_\nu(\mathbf{V}_s, \mathbf{V}_l(t))$. In this case, if the system is updated up to a time t and r_ν is a uniform random number in $[0, 1)$, we can set the time for the next ν event as the solution, τ_ν, to the equation [39]:

$$\int_t^{t+\tau_\nu} a_\nu(\mathbf{V}_s, \mathbf{V}_l(s))ds + \log(r_\nu) = 0 \tag{6}$$

It is well known that the stochastic formulation reduces to the deterministic formulation in the thermodynamic limit [40]. However, one important practical question is how large should the threshold M be to provide a satisfactory approximation in the implementation of the hybrid algorithm. In this article, we use a numerical criterion to determine this value. First, let $G(t)$ stand for the total number of cells of any of the cell types as a function of time (i.e. $G(t) = \sum X_i(t)$, $Y(t)$, $\sum Z_i(t)$, or $W(t)$). We can consider the function $E[G^{(M)}(t)]$ equal to the expected number of G type cells using the hybrid method with the threshold M. The L^2

norm (here denoted as $||\cdot||$) is a measure for the distance between two functions. We can then define the normalized error $\epsilon(M_1, M_2) = || E[G^{(M_1)}(t)] - E[G^{(M_2)}(t)] ||/|| E[G^{(M_2)}(t)] ||$, which provides a measure of the difference in the expected number of G cells using the two thresholds, M_1 and M_2, during a specific time interval I. To determine an acceptable threshold M, we define a tolerance tol and require that $\epsilon(M, 2M) < tol$. In the result section we discuss the accuracy of the approximation for the telomere model and improvements in the computational efficiency of the hybrid algorithm compared to a fully stochastic implementation (Figure 4 and Table 1).

Results

To study the effects of replicative limits and the emergence of double mutants ($p53^{+/-}$ and tmase+), we implement the model using a hybrid stochastic-deterministic algorithm detailed in the previous section of the paper.

Figures 2A-C plot simulations showing the three possible outcomes of the model. All simulations start with a single X type cell (tmase–, $p53^{+/+}$) with replication capacity $\rho_{\mathrm{m}} = 50$ (a commonly used value for human somatic cells [7]). Figure 2A depicts a simulation where a double mutation did not occur. In this panel the X population first rises to a value close the maximum population ($N = 10^7$), as the replication capacity of X cells is gradually exhausted X cells stop dividing, but continue to die, which leads to their eventual extinction. During the simulation $p53^{+/-}$ mutations take place, this allows Z cells to extend their replication capacity by ρ_e divisions. When Z cells exhaust their extended replication capacity, they become unstable and acquire the W cell phenotype, which is characterized by a high death rate D. Without the acquisition of a tmase+ mutation both the Z and W cell populations eventually go extinct. During this simulation tmase+ mutants do emerge (red line); however, because they do so at a time when most X cells have not exhausted their replication capacity they initially have no fitness advantage and in this simulation go stochastically extinct. Figure 2B depicts a simulation where a double mutant emerges from the Y cell population

(tmase+ followed by $p53^{+/-}$). The emergence of the double mutant is indicated by the red dot. Figure 2C plots a simulation where a double mutant emerges from the W cell population ($p53^{+/-}$ unstable followed by tmase+; purple dot).

Figure 2D plots the probability that the first double mutant emerges from the Y cell population (tmase+ first), calculated from those simulations where a double mutation occurred. The figure includes plots for two different values of the death rate, D, of W cells ($p53^{+/-}$ unstable), and two different values for the replication capacity extension, ρ_e, of Z cells. In the model the death rate for cells in crisis (W) must be greater than one, otherwise cells in crisis can go on dividing indefinitely, with ever shortening telomeres and increasing levels of chromosome instability (a scenario which is not biologically feasible). For this reason, we simulated two values for the death rate of W cells: $D = 1.05$, which represents a case where the death and birth rate are nearly balanced; and $D = 2$ (twice the size of the birth rate parameter r). Figure 2D also demonstrates that the size of the replication capacity extension, ρ_e, is crucial in determining the likelihood of the sequence of mutations (tmase+ followed by $p53^{+/-}$ vs. $p53^{+/-}$ followed by tmase+). Indeed, as shown in the simulations, a difference of only 10 cell division ($\rho_e = 20$ vs. $\rho_e = 30$) can dramatically alter the likelihood of the sequence of mutations. There is limited data for the value of ρ_e, although a range of 20–30 PD has been suggested [28, 29]. The actual value of ρ_e however, is in an all likelihood cell type dependent, and influenced by multiple factors, such as the level of telomere restriction factor two (TRF2) expression [3]. Note that for $D = 1.05$ (red lines), as d increases, there is a switch from $p53^{+/-}$ followed by tmase+ as the most likely sequence of mutations giving origin to the first double mutant, to tmase+ followed by $p53^{+/-}$. This behavior is explained by the fact that lower values of d allow for more Z cell divisions, which also result in higher W cell populations. The higher the number of Z and W cells, the more likely that the first double mutant originates in a $p53^{+/-}$ cell.

Figure 2E plots the probability of a double mutation occurring for different values of ρ_e and D. We note that the outcomes are sensitive to the value of ρ_e (red vs. blue lines). One

interesting result is that when there is no cell death of stable cells ($d = 0$), the probability of a double mutation occurring is basically zero. The reason why this occurs is that tmase+ mutations are only advantageous against a background of cells that senesce and die. Otherwise Y cells have a neutral fitness and are thus likely to go stochastically extinct. In a setting where X cells die, Y mutants might emerge and linger on until the time when they become advantageous, but without X cell death, Y cells never gain an advantage. Here and in all figures, we performed simulations up to a maximum time $T = 1000$ (relative to a division rate parameter $r = 1$). This value of T was sufficient for every simulation with $d > 0$ to result in either complete population extinction, or the emergence of a double mutant. This would not have been the case however, if we simulated very small positive values of d. To understand why, we note that if the simulated time was unbounded ($T = \infty$), the probability of a second mutation occurring would be monotonically decreasing for $d > 0$. Indeed, as d gets smaller, the average number of X cell divisions increases, and thus so does the probability of a double mutant emerging. However, as d decreases, the expected time of arrival of the first double mutant goes up (Figure 2F). In fact, by the arguments in the discussion of Figure 2F, it is straightforward to see that as d goes to zero, the expected arrival time of the first double mutant goes to infinity. Hence, for any finite time interval $[0, T]$, the probability of a second mutation emerging will not be monotonic for positive d, but instead will have the same basic shape as the plot in Figure 2E.

Figure 2F plots the time when a double mutation first emerges. In the simulations the mean arrival time of the first double mutant is not very sensitive to either the replication capacity extension, ρ_e, or the death rate of unstable cells, D. The reason why is that mutants are not selected for until X cells start becoming senescent. As soon as the number of X cells starts declining (the time of which is unaffected by ρ_e and D), pre-existing mutant clones gain an advantage, which can lead to the arrival of the first double mutant. In the simulations as $d > 0$ increases, there are on average fewer cell divisions, which means that the probability of a double mutation occurring goes down (Figure 2E). Higher d values also

cause X cells to become senescent sooner, which on average decreases the time at which mutants start to become advantageous. For this reason, even if higher values of d decrease the probability of a double mutation occurring, in those instances where a double mutation does happen, larger d values reduce the expected arrival time of the first double mutant (Figure 2F).

Figures 3A and 3B plot the probability that the first double mutant emerges from the unstable cell population (W), calculated from those instances where a double mutation occurred. As expected, decreasing the death rate of unstable cells increases the probability that the first double mutation originates in a W cell (dashed vs. solid lines). Also, increasing ρ_e by just 10 PD, from $\rho_e = 20$ to $\rho_e = 30$, significantly raises the likelihood that the first double mutant originates from an unstable cell. The dependence on d can be more nuanced. This is best exemplified by the curve corresponding to $\rho_e = 30$ and $D = 1.05$ (Figure 3B, solid line). While Figure 2D shows that the probability that the first double mutant originates in a $p53^{+/-}$ cell goes down as d increases, it is clear from Figure 3 that the likelihood that the the first double mutant emerges from the W cell population can be a non-monotonic function of d. The reason behind this behavior is that smaller values of d result in more Z and W cell divisions, making the emergence of the first double mutant from a $p53^{+/-}$ cell more likely; however, when the value of d is sufficiently small, the number of Z cells divisions can be large enough, so that the first double mutant can more often originate in Z cells directly, i.e., before $p53^{+/-}$ cells enter crisis.

Figures 3C and 3D present histograms depicting the distribution for the time of the first emergence of a double mutant, originating from two different sequence of events: tmase+ followed by $p53^{+/-}$, or $p53^{+/-}$ followed tmase+. The figure underscores the importance of the parameter ρ_e in determining the likelihood of the sequence of events. One interesting result is that, independent of the value of ρ_e, the expected time for the emergence of the first double mutant is smaller when the second mutation originates in the Y cell population. In other words, the average time of emergence of the first double mutation is faster when the

first mutation is tmase+.

Figure 4A plots the expected number of cells using the stochastic-deterministic thresholds $M = 2000$ (circles) and $M = 4000$ (solid lines), for simulations where double mutations did not occur –for all cell types depicted the normalized error $\epsilon(M, 2M) < 0.05$ over the time interval $I = [0, 1000]$. Figure 4B plots the distribution of the times when the first double mutant emerges, using a parameter set that makes the generation of a large number of fully stochastic independent trials computationally reasonable. This figure compares the results from a fully stochastic simulation algorithm with the results from an implementation of the hybrid method. Table 1 shows the average computational run time per trial for different max population sizes using the fully stochastic and the hybrid algorithm. For a maximum population size of $N = 10^7$ the hybrid algorithm is more than 2,200 times faster.

Discussion

Recently we presented a mathematical model with the aim of quantifying the effectiveness of replicative limits as a tumor suppressor pathway [41]. We also developed a Luria-Delbruck mutational framework to estimate the probability of escaping replicative limits through a mutation that activates telomerase [42]. These models assumed that the only constraint to cell proliferation was set by replicative limits. Here, we extend these results by studying the population dynamics in a setting where population size is also constrained by a fixed carrying capacity. We also consider the emergence of two of the most frequent events in tumorigenesis: Loss of p53 function and telomerase activation. The model has direct applications to an important telomerase negative mouse model and to p16 deficient human cells. Our work adds to growing body of literature that investigates mathematically the effects of replicative limits in cancer at the scale of cell populations (see e.g. [43, 44, 45]).

To implement our model we used a hybrid stochastic-deterministic algorithm. The algorithm simultaneously models large populations deterministically, and small populations and mutations stochastically. It provides good agreement with fully stochastic implementations

of the model, and very significant improvements in terms of speed (up to several orders of magnitude faster). These improvements in performance allows us to use biologically relevant population sizes and mutation rates, circumventing some of the traditional limitations of fully stochastic methods. The development of hybrid algorithms has received considerable attention in physical chemistry applications and related fields. These ideas however, have yet to find widespread use in the field of evolution. The hybrid methodology outlined in this paper could be easily adapted to model many aspects of tumor evolution, and more broadly, it can also be applied to a wide range of evolutionary models.

In this article we examined the relative frequency of the order of acquisition of the two mutations as a function of key biological parameters. We found that for any finite time interval, the probability of a double mutation occurring is a non-monotonic function of the death rate of stable cells (d). However, if we exclude very small values of d, then increasing the death rate of stable cells decreases the probability that a double mutation occurs. Our simulations also revealed that higher death rates of stable cells increase the likelihood that the first double mutant originates in a telomerase positive cell. The probability that the first double mutant emerges from an unstable cell has a more complex dependence on d. Indeed, depending on the sizes of the replication capacity extension of p53 mutants and the death rate of unstable cells, the probability that the first double mutation originates in an unstable cell can peak at intermediate values of d. We also found that the size of the replication capacity extension of p53 mutants is crucial in determining the probability of a double mutant occurring and the likelihood of the sequence of mutations. In particular, we found that a difference of just ten population doublings in the replication capacity extension can significantly impact the behavior of the system. Interestingly, the expected arrival time of the first double mutant is only weakly dependent on the replication capacity extension and the death rate of unstable cells. Instead it is most influenced by the time at which the telomerase negative p53 wild-type cell population starts to senesce, since only then do pre-existing mutants become advantageous.

Compared to sarcomas and hematopoietic malignancies, epithelial cancers require a large number of mutations and genome rearrangements to achieve a malignant state [46]. It has thus been suggested that a mutator phenotype must take place to account for the constellation of genome abnormalities found in many malignant carcinomas. In this respect, telomere-based crisis has been identified as a key mutator mechanism driving epithelial carcinogenesis in cells that initially lack telomerase [3]. Here we presented a mathematical model that takes into account replicative limits and examines the dynamics of two mutations central to the entrance and escape from crisis. One important extension to the model will be the inclusion of mutational events, such as translocations and loss of heterozygosity (LOH), which occur at increased rates during crisis. In particular, this will require modeling the population dynamics and possible fitness differences between different types of double mutants. This analysis will be fundamental to understand quantitatively under which conditions telomere shortening shifts from being a powerful tumor suppressor pathway to a driving force behind carcinogenesis.

Figure legends

Figure 1. (A) Each cell has a replication capacity $\rho \geq 0$. When a cell with replication capacity $\rho > 0$ divides, it produces two daughter cells with replication capacities $\rho - 1$. Cells with replication capacity $\rho = 0$ become senescent and stop dividing. (B) Different pathways by which cells can acquire two cancer associated mutations: Activation of telomerase (tmase+) and inactivation of one p53 allele ($p53^{+/-}$). The mutation rate for acquiring the $p53^{+/-}$ phenotype is set to $\mu_1 = 10^{-7}$ (loss of one tumor suppressor allele). The mutation rate to activate telomerase is set to $\mu_2 = 10^{-9}$ (point mutation). $p53^{+/-}$ cells have a defective DNA damage response, which allows them to undergo extra rounds of cell division beyond the normal replication capacity ρ. In $p53^{+/-}$ cells telomere length continues to decrease with each cell division, eventually leading to telomere crisis. Crisis is characterized by critically short telomeres causing chromosome breakage–fusion–bridge cycles and widespread cell

death. Cells in crisis are referred in the diagram as $p53^{+/-}$ unstable cells. Telomerase activation allows cells to escape replication limits, making them capable of dividing an unlimited number of times.

Figure 2. Times series of a simulation when: (A) a double mutation never occurs; (B) the first mutation emerges from Y cell population (tmase+ first); and (C), the first mutation emerges from the W cell population ($p53^{+/-}$ first). In each panel, the first emergence of a double mutation is indicated by s solid dot. In panels A–C, $\rho_e = 20, d = 0.1,$ and, $D = 1.05$. (D) Probability that the first double mutant emerges through the pathway tmase+ first followed by $p53^{+/-}$. Error bars indicate 95% confidence intervals. Blue and red colors correspond to different values of the replication capacity extension ρ_e, defined as the number of extra division that $p53^{+/-}$ cells can undergo before entering crisis. Solid and dashed lines indicate different values D for the cell death of unstable cells (compared to a dimensionless division rate parameter $r = 1$). The maximum replication capacity of of X cells (tmase– and $p53^{+/+}$) is set to $\rho_m = 50$. (E) Probability of the emergence of a double mutant. (F) Expected time of the first emergence of a double mutant. Results based on $10^5 - 10^6$ simulations per data point.

Figure 3. (A) and (B): Probability that the first double mutant emerges from the population of unstable (W) cells –conditioning over those instances where a double mutation occurred. Two different death rates of unstable cells are depicted, $D = 1.05$ (solid lines) and $D = 2$ (dashed lines). (C) and (D): Distribution of the arrival time of the first double mutant. The panels correspond to two different values of the replication capacity extension ρ_e, defined as the number of extra division that $p53^{+/-}$ cells can undergo before entering crisis. In (A) and (C) $\rho_e = 20$; in (B) and (D) $\rho_e = 30$. In all panels $\rho_m = 50$. In (C) and (D), $d = 0.1$ and $D = 1.05$.

Figure 4. (A) Expected number of cells using two different thresholds, M, for the size that determines the stochastic to deterministic transition. Solid lines $M = 2000$; circles

$M = 4000$. The panel corresponds to simulations where a double mutant did not emerge. Parameters: $\rho_{\mathrm{m}} = 50, \rho_{\mathrm{e}} = 20, d = 0.1,$ and $D = 1.05$. (B) Distribution of the arrival time of the first double mutant for a parameter set that makes the generation of a large number of fully stochastic independent trials computationally reasonable. Blue: Results from fully stochastic simulations. Red: Results using the hybrid method. Parameters: $K = 10^4$, $\mu_1 = 10^{-4}$, $\mu_2 = 10^{-6}$, $\rho_{\mathrm{m}} = 30$, $\rho_{\mathrm{e}} = 15$, $d = 0.1$, and $D = 1.05$.

References

[1] Mel Greaves. *Cancer: the evolutionary legacy*. Oxford University Press on Demand, 2001.

[2] Steven A Frank. *Dynamics of cancer: incidence, inheritance, and evolution*. Princeton University Press, 2007.

[3] John Maciejowski and Titia de Lange. Telomeres in cancer: tumour suppression and genome instability. *Nat Rev Mol Cell Biol*, 18(3):175–186, Mar 2017. doi: 10.1038/nrm.2016.171.

[4] Ignacio A Rodriguez-Brenes and Dominik Wodarz. Preventing clonal evolutionary processes in cancer: Insights from mathematical models. *Proc Natl Acad Sci U S A*, 112 (29):8843–50, Jul 2015. doi: 10.1073/pnas.1501730112.

[5] A Daniel Gillespie. General method for numerically simulating the stochastic time evolution of coupled chemical reactions. *Journal of computational physics*, 22, 1976.

[6] Jerry W Shay and Woodring E Wright. Senescence and immortalization: role of telomeres and telomerase. *Carcinogenesis*, 26(5):867–74, May 2005. doi: 10.1093/carcin/bgh296.

[7] L Hayflick. The limited in vitro lifetime of human diploid cell strains. *Exp Cell Res*, 37: 614–36, Mar 1965.

[8] Koei Chin, Carlos Ortiz de Solorzano, David Knowles, Arthur Jones, William Chou, Enrique Garcia Rodriguez, Wen-Lin Kuo, Britt-Marie Ljung, Karen Chew, Kenneth Myambo, Monica Miranda, Sheryl Krig, James Garbe, Martha Stampfer, Paul Yaswen, Joe W Gray, and Stephen J Lockett. In situ analyses of genome instability in breast cancer. *Nat Genet*, 36(9):984–8, Sep 2004. doi: 10.1038/ng1409.

[9] Audrey Petitjean, Ewy Mathe, Shunsuke Kato, Chikashi Ishioka, Sean V Tavtigian, Pierre Hainaut, and Magali Olivier. Impact of mutant p53 functional properties on tp53 mutation patterns and tumor phenotype: lessons from recent developments in the iarc tp53 database. *Hum Mutat*, 28(6):622–9, Jun 2007. doi: 10.1002/humu.20495.

[10] Jacqueline J L Jacobs and Titia de Lange. Significant role for p16ink4a in p53-independent telomere-directed senescence. *Curr Biol*, 14(24):2302–8, Dec 2004. doi: 10.1016/j.cub.2004.12.025.

[11] Manuel Collado, Maria A Blasco, and Manuel Serrano. Cellular senescence in cancer and aging. *Cell*, 130(2):223–233, 2007.

[12] M A Blasco, H W Lee, M P Hande, E Samper, P M Lansdorp, R A DePinho, and C W Greider. Telomere shortening and tumor formation by mouse cells lacking telomerase rna. *Cell*, 91(1):25–34, Oct 1997.

[13] R A Greenberg, L Chin, A Femino, K H Lee, G J Gottlieb, R H Singer, C W Greider, and R A DePinho. Short dysfunctional telomeres impair tumorigenesis in the ink4a(delta2/3) cancer-prone mouse. *Cell*, 97(4):515–25, May 1999.

[14] Christine M Khoo, Daniel R Carrasco, Marcus W Bosenberg, Ji-Hye Paik, and Ronald A Depinho. Ink4a/arf tumor suppressor does not modulate the degenerative conditions or tumor spectrum of the telomerase-deficient mouse. *Proc Natl Acad Sci U S A*, 104(10): 3931–6, Mar 2007. doi: 10.1073/pnas.0700093104.

[15] Agata Smogorzewska and Titia de Lange. Different telomere damage signaling pathways in human and mouse cells. *EMBO J*, 21(16):4338–48, Aug 2002.

[16] S E Artandi, S Chang, S L Lee, S Alson, G J Gottlieb, L Chin, and R A DePinho. Telomere dysfunction promotes non-reciprocal translocations and epithelial cancers in mice. *Nature*, 406(6796):641–5, Aug 2000. doi: 10.1038/35020592.

[17] N W Kim, M A Piatyszek, K R Prowse, C B Harley, M D West, P L Ho, G M Coviello, W E Wright, S L Weinrich, and J W Shay. Specific association of human telomerase activity with immortal cells and cancer. *Science*, 266(5193):2011–5, Dec 1994.

[18] Utz Herbig, Wendy A Jobling, Benjamin PC Chen, David J Chen, and John M Sedivy. Telomere shortening triggers senescence of human cells through a pathway involving atm, p53, and p21 cip1, but not p16 ink4a. *Molecular cell*, 14(4):501–513, 2004.

[19] Charles R Holst, Gerard J Nuovo, Manel Esteller, Karen Chew, Stephen B Baylin, James G Herman, and Thea D Tlsty. Methylation of p16(ink4a) promoters occurs in vivo in histologically normal human mammary epithelia. *Cancer Res*, 63(7):1596–601, Apr 2003.

[20] S R Romanov, B K Kozakiewicz, C R Holst, M R Stampfer, L M Haupt, and T D Tlsty. Normal human mammary epithelial cells spontaneously escape senescence and acquire genomic changes. *Nature*, 409(6820):633–7, Feb 2001. doi: 10.1038/35054579.

[21] Purificación Feijoo, Mariona Terradas, David Soler, Daniel Domínguez, Laura Tusell, and Anna Genescà. Breast primary epithelial cells that escape p16-dependent stasis enter a telomere-driven crisis state. *Breast Cancer Research*, 18(1):7, 2016.

[22] F W Huang, C M Bielski, M L Rinne, W C Hahn, W R Sellers, F Stegmeier, L A Garraway, and G V Kryukov. Tert promoter mutations and monoallelic activation of tert in cancer. *Oncogenesis*, 4:e176, Dec 2015. doi: 10.1038/oncsis.2015.39.

[23] Franklin W Huang, Eran Hodis, Mary Jue Xu, Gregory V Kryukov, Lynda Chin, and Levi A Garraway. Highly recurrent tert promoter mutations in human melanoma. *Science*, 339(6122):957–9, Feb 2013. doi: 10.1126/science.1229259.

[24] Patrick J Killela, Zachary J Reitman, Yuchen Jiao, Chetan Bettegowda, Nishant Agrawal, Luis A Diaz, Allan H Friedman, Henry Friedman, Gary L Gallia, Beppino C Giovanella, et al. Tert promoter mutations occur frequently in gliomas and a subset of tumors derived from cells with low rates of self-renewal. *Proceedings of the National Academy of Sciences*, 110(15):6021–6026, 2013.

[25] Jean Charles Nault, Maxime Mallet, Camilla Pilati, Julien Calderaro, Paulette Bioulac-Sage, Christophe Laurent, Alexis Laurent, Daniel Cherqui, Charles Balabaud, Jessica Zucman-Rossi, and Jessica Zucman Rossi. High frequency of telomerase reverse-transcriptase promoter somatic mutations in hepatocellular carcinoma and preneoplastic lesions. *Nat Commun*, 4:2218, 2013. doi: 10.1038/ncomms3218.

[26] Siân Jones, Wei-Dong Chen, Giovanni Parmigiani, Frank Diehl, Niko Beerenwinkel, Tibor Antal, Arne Traulsen, Martin A Nowak, Christopher Siegel, Victor E Velculescu, Kenneth W Kinzler, Bert Vogelstein, Joseph Willis, and Sanford D Markowitz. Comparative lesion sequencing provides insights into tumor evolution. *Proc Natl Acad Sci U S A*, 105(11):4283–8, Mar 2008. doi: 10.1073/pnas.0712345105.

[27] Alice H Berger and Pier Paolo Pandolfi. Haplo-insufficiency: a driving force in cancer. *J Pathol*, 223(2):137–46, Jan 2011. doi: 10.1002/path.2800.

[28] T M Bryan and R R Reddel. Sv40-induced immortalization of human cells. *Crit Rev Oncog*, 5(4):331–57, 1994.

[29] Ramiro E Verdun and Jan Karlseder. Replication and protection of telomeres. *Nature*, 447(7147):924–31, Jun 2007. doi: 10.1038/nature05976.

[30] Natalia L Komarova, Anirvan Sengupta, and Martin A Nowak. Mutation-selection

networks of cancer initiation: tumor suppressor genes and chromosomal instability. *J Theor Biol*, 223(4):433–50, Aug 2003.

[31] K L Rudolph, M Millard, M W Bosenberg, and R A DePinho. Telomere dysfunction and evolution of intestinal carcinoma in mice and humans. *Nat Genet*, 28(2):155–9, Jun 2001. doi: 10.1038/88871.

[32] I M Shih, W Zhou, S N Goodman, C Lengauer, K W Kinzler, and B Vogelstein. Evidence that genetic instability occurs at an early stage of colorectal tumorigenesis. *Cancer Res*, 61(3):818–22, Feb 2001.

[33] F A Tavassoli and H J Norris. A comparison of the results of long-term follow-up for atypical intraductal hyperplasia and intraductal hyperplasia of the breast. *Cancer*, 65 (3):518–29, Feb 1990.

[34] Judah Folkman. Tumor angiogenesis: therapeutic implications. *New england journal of medicine*, 285(21):1182–1186, 1971.

[35] Frank A W Coumans, Guus van Dalum, Markus Beck, and Leon W M M Terstappen. Filter characteristics influencing circulating tumor cell enrichment from whole blood. *PLoS One*, 8(4):e61770, 2013. doi: 10.1371/journal.pone.0061770.

[36] Michael A Gibson and Jehoshua Bruck. Efficient exact stochastic simulation of chemical systems with many species and many channels. *The journal of physical chemistry A*, 104(9):1876–1889, 2000.

[37] Yang Cao, Daniel T Gillespie, and Linda R Petzold. Efficient step size selection for the tau-leaping simulation method. *J Chem Phys*, 124(4):044109, Jan 2006. doi: 10.1063/1.2159468.

[38] Eric L Haseltine and James B Rawlings. Approximate simulation of coupled fast and slow reactions for stochastic chemical kinetics. *The Journal of chemical physics*, 117 (15):6959–6969, 2002.

[39] Howard Salis and Yiannis Kaznessis. Accurate hybrid stochastic simulation of a system of coupled chemical or biochemical reactions. *The Journal of chemical physics*, 122(5): 054103, 2005.

[40] Thomas G Kurtz. The relationship between stochastic and deterministic models for chemical reactions. *The Journal of Chemical Physics*, 57(7):2976–2978, 1972.

[41] Ignacio A Rodriguez-Brenes, Dominik Wodarz, and Natalia L Komarova. Quantifying replicative senescence as a tumor suppressor pathway and a target for cancer therapy. *Sci Rep*, 5:17660, Dec 2015. doi: 10.1038/srep17660.

[42] Ignacio A Rodriguez-Brenes, Dominik Wodarz, and Natalia L Komarova. Cellular replication limits in the luria–delbrück mutation model. *Physica D: Nonlinear Phenomena*, 328:44–51, 2016.

[43] Heiko Enderling, Alexander R A Anderson, Mark A J Chaplain, Afshin Beheshti, Lynn Hlatky, and Philip Hahnfeldt. Paradoxical dependencies of tumor dormancy and progression on basic cell kinetics. *Cancer Res*, 69(22):8814–21, Nov 2009. doi: 10.1158/0008-5472.CAN-09-2115.

[44] Ignacio A Rodriguez-Brenes, Dominik Wodarz, and Natalia L Komarova. Minimizing the risk of cancer: tissue architecture and cellular replication limits. *J R Soc Interface*, 10(86):20130410, Sep 2013. doi: 10.1098/rsif.2013.0410.

[45] Ignacio A Rodriguez-Brenes, Natalia L Komarova, and Dominik Wodarz. Cancer-associated mutations in healthy individuals: assessing the risk of carcinogenesis. *Cancer research*, 74(6):1661–1669, 2014.

[46] Steven E Artandi and Ronald A DePinho. Telomeres and telomerase in cancer. *Carcinogenesis*, 31(1):9–18, 2010.

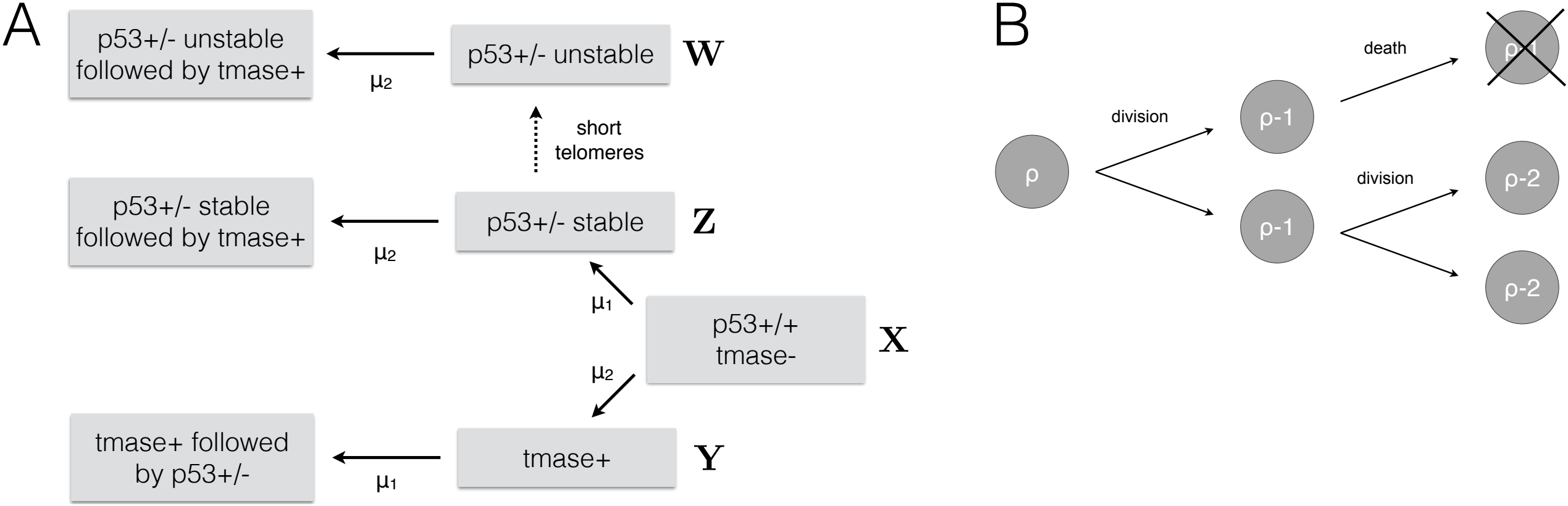
A
p53+/- unstable followed by tmase+
μ2
p53+/- unstable
W
short telomeres
p53+/- stable followed by tmase+
μ2
p53+/- stable
Z
μ1
p53+/+ tmase-
X
μ2
tmase+ followed by p53+/-
μ1
tmase+
Y
B
ρ
division
ρ-1
ρ-1
death
division
ρ-2
ρ-2

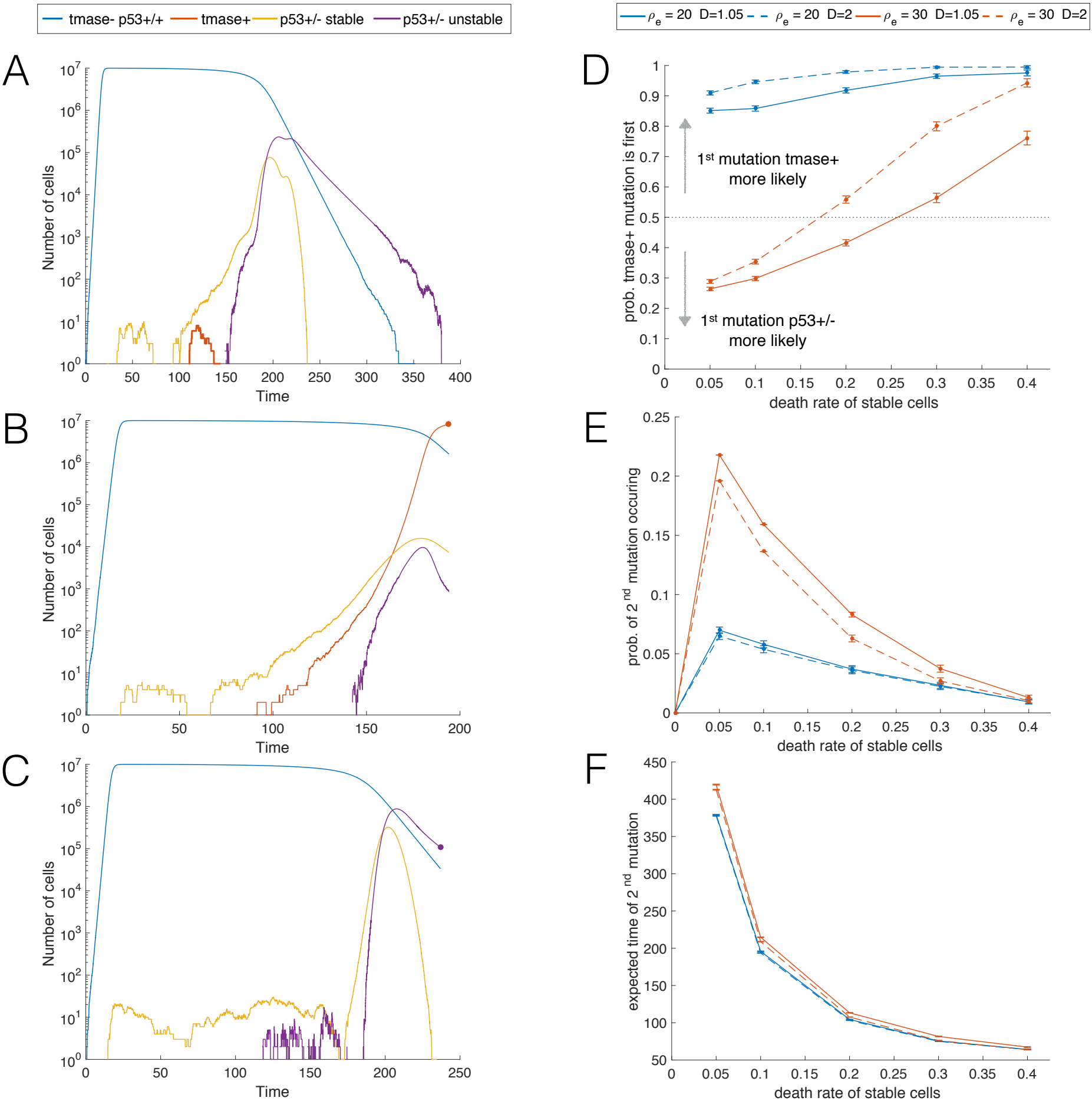
tmase- p53+/+
tmase+
p53+/- stable
p53+/- unstable
A
Number of cells
Time
B
Number of cells
Time
C
Number of cells
Time
ρ_e = 20 D=1.05
ρ_e = 20 D=2
ρ_e = 30 D=1.05
ρ_e = 30 D=2
D
prob. tmase+ mutation is first
1st mutation tmase+ more likely
1st mutation p53+/- more likely
death rate of stable cells
E
prob. of 2nd mutation occuring
death rate of stable cells
F
expected time of 2nd mutation
death rate of stable cells

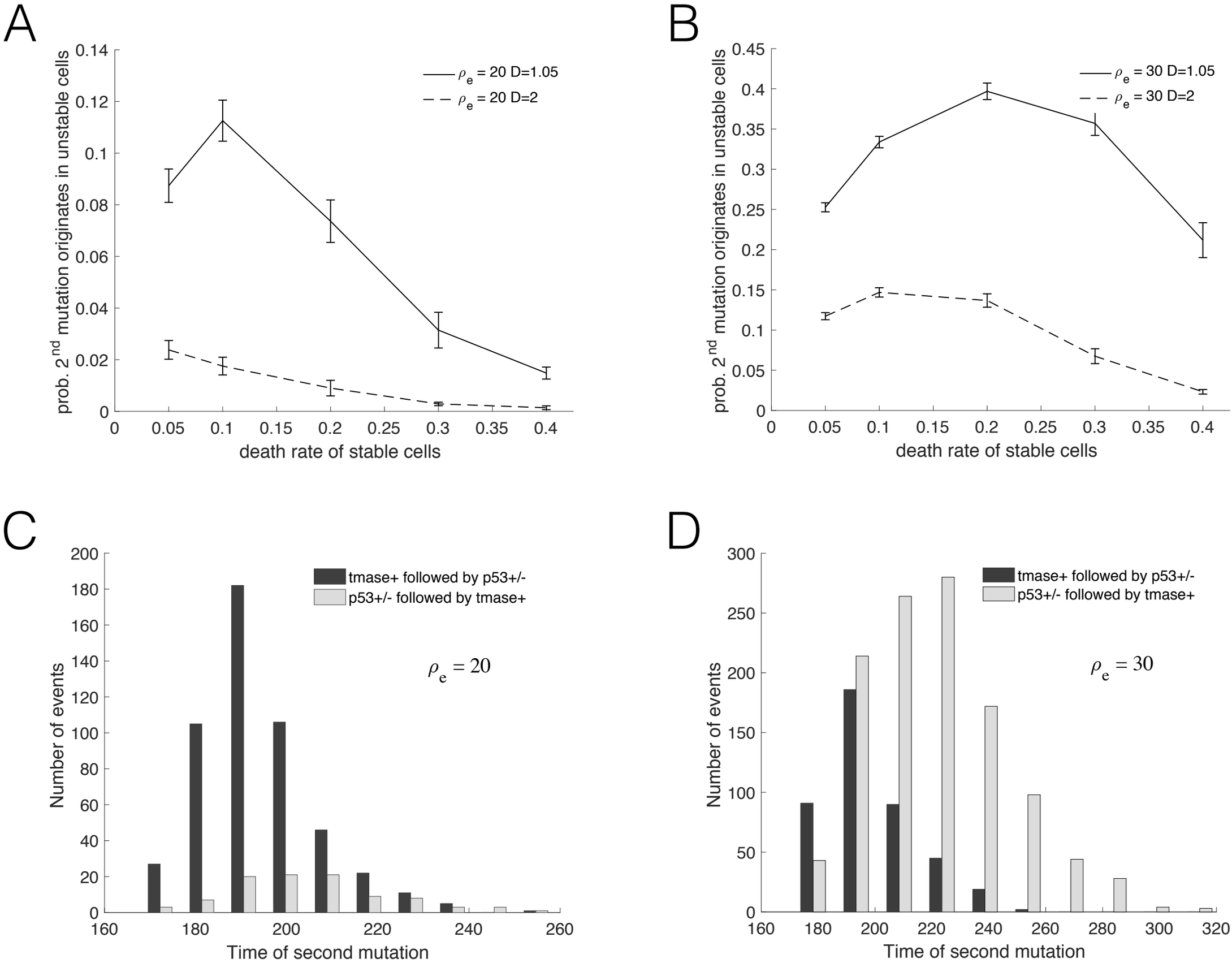
A
B
C
D
prob. 2nd mutation originates in unstable cells
death rate of stable cells
ρe = 20 D=1.05
ρe = 20 D=2
ρe = 30 D=1.05
ρe = 30 D=2
Number of events
Time of second mutation
tmase+ followed by p53+/-
p53+/- followed by tmase+
ρe = 20
ρe = 30

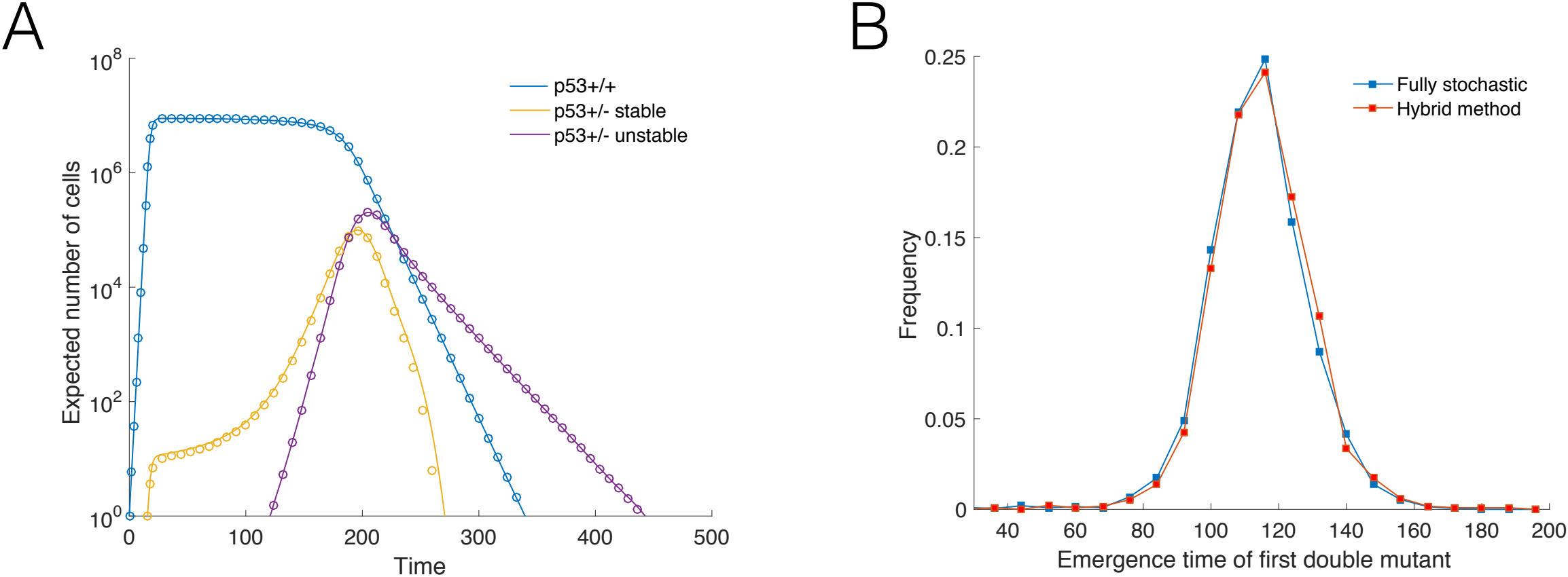
A
B
Expected number of cells
Time
p53+/+
p53+/- stable
p53+/- unstable
Frequency
Emergence time of first double mutant
Fully stochastic
Hybrid method

TABLE I. Execution time.

Max Population Size	Hybrid (s)	Fully Stochastic (s)
10 000	0.10	0.76
100 000	0.11	6.55
1 000 000	0.12	58.47
10 000 000	0.22	503.39